

# Analysis of Channel Stress Induced by NiPt-silicide and Its Generation Mechanism

Mariko Mizuo<sup>1</sup>, Tadashi Yamaguchi<sup>2</sup>, Shuichi Kudo<sup>2</sup>, Yukinori Hirose<sup>1,2</sup>, Hiroshi Kimura<sup>2</sup>,  
Jun-ichi Tsuchimoto<sup>2</sup> and Nobuyoshi Hattori<sup>2</sup>

<sup>1</sup>Renesas Semiconductor Engineering Corp., Process Integration Engineering Department, 4-1-3, Mizuhara, Itami, Hyogo 664-0005, Japan

<sup>2</sup>Renesas Electronics Corp., Devices & Analysis Technology Division, 4-1-3, Mizuhara, Itami, Hyogo 664-0005, Japan,

Phone: +81-72-787-5939 E-mail: mariko.mizuo.rh@rse.renesas.com

## 1. Introduction

Stress control techniques of the channel region have been actively used to enhance carrier mobility of MOS-FETs. Naturally, the stress control of silicide film on the source/drain (S/D) region is also quite important for high performance transistors. NiPt-silicide has been applied to advanced MOSFETs, and it has been reported that the NiPt-silicide film has tensile stress [1]. However, the influence of NiPt silicide on the channel stress has not been sufficiently investigated yet.

For analyzing strain at localized transistor area, transmission electron microscopy has been proposed, however the stress relaxation is inevitable during thin sample-preparations [2]. In contrast, Raman spectroscopy is a powerful tool for channel-stress measurement without sample destruction. Furthermore, the Raman spectroscopy using the UV laser with 363.8 nm wavelength is sensitive to the Si surface because its half penetration depth in Si is quite shallow (~ 5 nm).

In this paper, we demonstrated the channel stress induced by NiPt-silicide using UV Raman spectroscopy. Furthermore, we revealed the influences on the channel stress of annealing methods for silicide formation and P- or N-type S/D, by analyzing microstructures in silicide using x-ray diffraction (XRD). Consequently, we propose the generation mechanism of channel-stress.

## 2. Experimental Procedure

Figure 1 shows the test structure [3]. The stress at the channel region was measured by UV Raman spectroscopy using these structures. Figure 2 shows the schematic process flow of sample preparation. In the particular test structure, NiPt-silicide was formed on P-type and N-type S/D. In the 2<sup>nd</sup> annealing, we have three kinds of annealing methods; conventional rapid thermal annealing (RTA), laser annealing (LA), and microwave annealing (MWA).

In order to discuss the generation mechanism of channel stress, we also prepared blanket NiPt-silicide films on (001)-oriented Si substrate for XRD measurement, which was performed using Cu K $\alpha$  source.

## 3. Results and discussions

### Measurement of channel stress by UV Raman spectroscopy

Figure 3 shows the result of the channel stress as a function of SiO<sub>2</sub>-gate length (L<sub>g</sub>) before and after NiPt-silicide formed by RTA. Before silicide formation, compressive stress less than 30 MPa was applied to the channel region with every L<sub>g</sub> pattern. After the silicide formation, tensile stress is induced at each channel region, and the stress in-

tensity increases as L<sub>g</sub> narrows. It is concluded that the channel stress can be successfully measured by UV Raman spectroscopy with the Raman test structure.

Figure 4 shows the stress at the channel region of 200 nm L<sub>g</sub> as a function of 2<sup>nd</sup> annealing methods. The tensile stress of channel region for P-type S/D sample was higher than that for N-type S/D sample with every 2<sup>nd</sup> annealing method. Furthermore, it is clear that the channel stress strongly depends on 2<sup>nd</sup> annealing process conditions.

### Microstructure analyses of NiPt-silicide films

NiSi is known to have an orthorhombic MnP- type crystal structure [4]. Figure 5 shows the results of measured NiPt-silicide crystal orientation to the Si[001] direction by out-of-plane XRD. Peaks of NiSi(020) and NiSi(013) planes and the peak shift from the value of strain-free condition were observed [4]. The peak shifts indicate NiSi lattice space changing ( $\Delta d$ ), which means the strain of NiPt-silicide.  $\Delta d$  of NiSi(020) and NiSi(013) with each 2<sup>nd</sup> annealing method are shown in Fig. 6. The value of  $\Delta d$  of NiSi(020) was larger than that of NiSi(013), especially with LA. Furthermore, the peak intensity of NiSi(020) in P-type film was higher than that in N-type film as shown in Fig. 7. Consequently, peak intensity of NiSi(101), (002), (200), (102) and (103) through in-plane XRD in P-type film was higher than that in N-type film as shown in Fig. 8. Focusing on  $\Delta d$  of NiSi(200) in Fig. 9,  $\Delta d$  in P-type film was larger than that in N-type film. Moreover,  $\Delta d$  of LA was larger than that of RTA and MWA.

### Generation mechanism of channel stress

Figure 10 shows the NiSi lattice constants of three (a-, b-, c-) axes, based on coefficient of thermal expansion (CTE) [5]. The b-axis of NiSi grains contract due to negative CTE, and the a- and c-axes of NiSi grains expand due to a large positive CTE. Figure 11 shows the schematics of the stress generation model. The NiPt-silicide grains along b-axis to Si[001] were deformed after annealing [see Green and Black lines in Fig. 11(a)]. As the a- and c-axes in NiSi have larger positive CTE compared with the Si substrates, residual stress in NiPt-silicide generates after annealing. This residual stress expands Si lattice at channel regions as shown in Fig. 11(b). This model suggests that low temperature annealing and the reduction of NiSi grains along the b-axis to Si[001] suppresses the residual stress in NiPt-silicide.

## 4. Conclusions

The channel stress induced by NiPt-silicide was investigated with UV Raman spectroscopy and its generation

mechanism was revealed with XRD. The stress generation mechanism can be explained by the crystal orientations of NiSi film and the lattice parameter alteration of NiSi film as a function of temperature. These analyses are quite valuable to promotion of stress-control engineering for high performance CMOS transistors.

## References

- [1] C. Detavemier et al., Appl. Phys. Lett. 84, 3549(2004).
- [2] D. Kosemura et al., Jpn J. Appl. Phys. 50 (2011)04DA06.
- [3] T. Yamaguchi et al., Jpn J. Appl. Phys. 50 (2011)04DA02.
- [4] Joint Committee on Powder Diffraction Standards 38-0844.
- [5] D. F. Wilson et al., Scr. Metall. Mater. 26, 85 (1992).

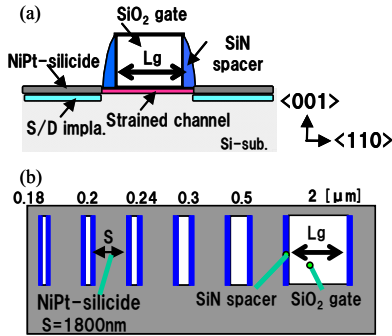


Fig. 1. Schematic diagrams of Raman test structure. (a) Cross-sectional view. (b) Plan view.

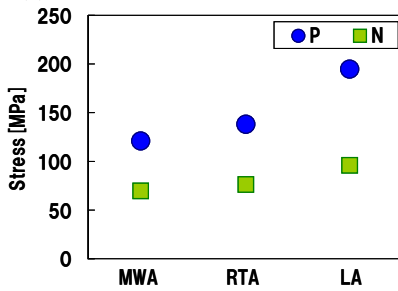


Fig. 4. Raman results ( $L_g=200\text{nm}$ ) depending on 2<sup>nd</sup> annealing methods.

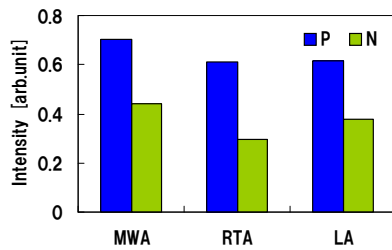


Fig. 7. Measurement results of peak intensity of NiSi (020) with out-of-plane XRD.

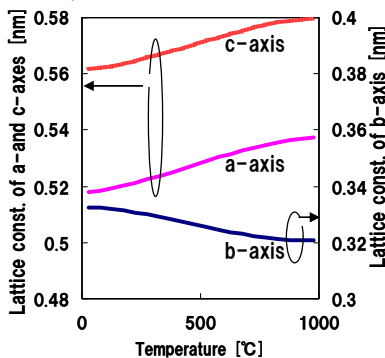


Fig. 10. NiSi lattice constants of three (a-, b-, c-) axes as a function of temperature.

- SiO<sub>2</sub> gate formation
- Sidewall formation
- S/D implantation & activation  
P-type (B,Ge) /N-type (As ,P)
- NiPt deposition
- 1<sup>st</sup> annealing; Conventional RTA (260 °C)
- Un-reacted NiPt selective etching
- 2<sup>nd</sup> annealing;
  - microwave annealing (MWA) (< 250 °C)
  - rapid thermal annealing (RTA) (525 °C)
  - laser annealing (LA) (900 °C)

Fig. 2. Schematic process flow of sample preparation.

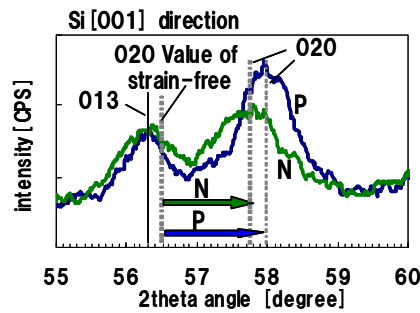


Fig. 5. Out-of-plane XRD results for NiPt-silicide films with LA.

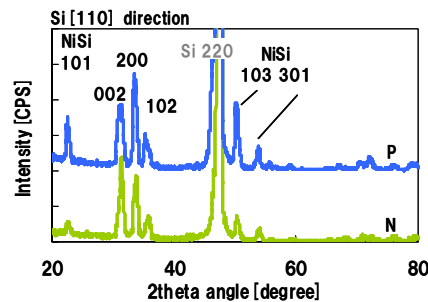


Fig. 8. In-plane XRD results for NiPt-silicide films with LA.

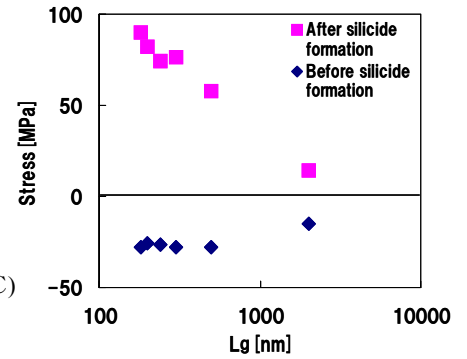


Fig. 3. Stress measurement results on variation of  $L_g$  by Raman. (2<sup>nd</sup> annealing; RTA).

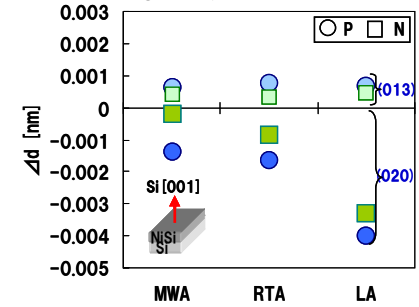


Fig. 6.  $\Delta d$  of NiSi(013) and NiSi(020) derived from Fig. 5.

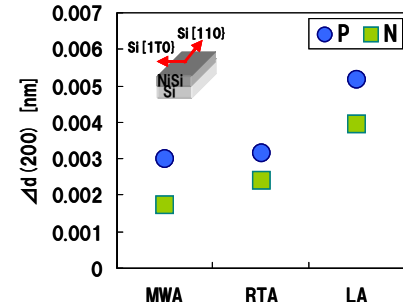


Fig. 9.  $\Delta d$  of NiSi(200) derived from Fig. 8. (Si<110> direction)

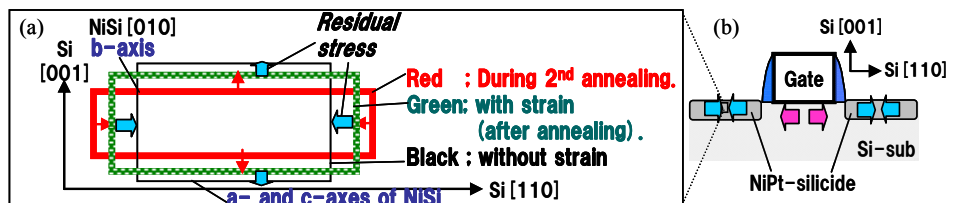


Fig. 11. Schematic drawing of channel stress generation model.